International Journal of Mass Spectrometry and Ion Physics, 26 (1978) 23—38

PHOTOIONIZATION AND THRESHOLD PHOTOELECTRON–PHOTOION COINCIDENCE STUDY OF ALLENE FROM ONSET TO 20 eV

ALBERT C. PARR and ANDREW J. JASON

Department of Physics and Astronomy, The University of Alabama, Alabama 35486 (U.S.A.)

ROGER STOCKBAUER

Institute for Materials Research, National Bureau of Standards, Washington, DC 20234 (U.S.A.)

(Received 19 April 1977)

ABSTRACT

The photoionization efficiency curves for allene and its fragments $C_3H_3^+$, $C_3H_2^+$ and C_3H^+ are given from threshold to 20 eV. The threshold photoelectron spectra and breakdown curves are given over the same energy span. The adiabatic ionization potential is determined to be 9.69 ± 0.01 eV and the heats of formation of the fragments are derived from the appearance potentials. Autoionization is found to be an important factor in the parent ionization and fragmentation.

INTRODUCTION

Sutcliffe and Walsh [1] photographed the absorption spectrum of allene in the wavelength region 1250—2100 Å. They found absorption bands and fitted a number of them to Rydberg series leading to a presumably vertical ionization potential of 10.19 ± 0.01 eV. More recent spectroscopic work by Iverson and Russell [2] has confirmed some of the interpretations of Sutcliffe and Walsh and suggested refinements in others. They found two major Rydberg series which converged to an ionization potential 10.016 ± 0.002 eV. Rabalais et al. [3] studied allene absorption over approximately the same wavelength region as Iverson and Russell. They identify three main Rydberg series of type $\pi \rightarrow ns$, $\pi \rightarrow np$ and $\pi \rightarrow nd$ transitions with a limit of 10.19 ± 0.01 eV. The series listed by Iverson and Russell are different from those listed by Rabalais et al., each having different energy levels and quantum defects. Herzberg [4] pointed out that some of the fragmentary Rydberg series listed by Sutcliffe and Walsh were probably vibrational members of other series. Sutcliffe and Walsh's work was reinterpreted by Betts and McKoy [5] and a more consistent set of assignments made.

Baker and Turner [6] studied allene using 584-Å photoelectron spectroscopy (PES). They found an adiabatic ionization potential of 9.69 eV and gave a value 10.0 eV for the vertical ionization energy. In addition they found evidence suggestive of Jahn—Teller splitting in the ionic ground state and have located several excited states of the ion. Thomas and Thompson [7], using PES, reported a value of 9.68 eV for the adiabatic ionization potential and values for vertical ionization potentials of 10.02, 14.75 and 17.3 eV.

A photoionization study by Parr and Elder [8] suggested an adiabatic ionization potential of 9.62 ± 0.04 eV. The intensity at onset was small, however, making interpretation difficult. Above 10 eV, the ionization efficiency curve showed a great deal of structure characteristic of autoionization. The step structure that would be expected from comparison with photoelectron spectroscopic results is absent. The implication is, hence, that the photoionization cross-section of the allene molecule in this energy region, i.e. above 10 eV, is dominated by autoionization. Since this autoionization has not been studied in detail we feel that photoionization efficiency curves at higher resolution will provide data which will be useful in characterizing these upper states.

The $C_3H_3^+$ fragment of allene has been studied by Parr and Elder [8], and Matthews and Warneck [9] using photoionization and by Lossing [10] using monoenergetic electron impact. These studies were largely confined to the threshold region. An earlier electron impact study by Franklin and Mogenis [11] reported appearance potential for the higher-energy fragments but their results for the parent and $C_3H_3^+$ fragment are not in agreement with the more recent photoionization [8,9] and electron monochromator [10] studies.

Since allene is a relatively small molecule and its fragmentation relatively simple (there is no C—C bond breaking below 20 eV), its fragmentation should be fairly simple to calculate using the quasi-equilibrium theory (QET) [12]. Because fragmentation data obtained with recently developed photoelectron—photoion coincidence techniques [13] can be compared directly with such calculations, it appears worthwhile to provide such data.

EXPERIMENTAL

The photoionization experiments were performed on a photoionization mass spectrometer consisting of a 1-m focal length Seya—Namioka monochromator and a 3-in radius of curvature magnetic sector mass analyzer. The monochromator is windowless and is differentially pumped so that pressures in the ion source region are in the 10^{-6}-torr range when the light source is operating. The hydrogen many-line spectrum was generated by a d.c. discharge in hydrogen and the Hopfield continuum is generated with a pulsed discharge in helium. These sources give usable wavelengths from 600 Å to 2000 Å.

After magnetic deflection the ions are detected with a continuous channel

electron multiplier. The individual ions are counted with an electronic scaling system and light intensity is monitored with a sodium salicylate coated photomultiplier. The ion count divided by the light intensity gives the photoionization efficiency curves.

The resolution of the monochromator was ca. 2 Å for the photoionization data reported here. This resolution is approximately a factor of 2 better than the resolution of the previous photoionization results [8] and the data are in general the same over the regions where comparison is possible. The previous work reported results only to ca. 13 eV whereas the present paper gives results to ca. 20 eV. The previous work showed the general features of autoionization reported here although not in such a pronounced manner. The differences in peak heights are due to differences in data point density and to the higher resolution of the monochromator.

The threshold photoelectron spectra (TPES) and breakdown curves were measured on a threshold photoelectron—photoion coincidence mass spectrometer recently completed at the National Bureau of Standards. The instrument has been previously described [14]. The mass resolution of the instrument was increased to ca. 80 by increasing the ion drawout pulse voltage and using time lag focusing [15]. The hydrogen many-line spectrum and the Hopfield continuum of helium were used as light sources. The electrons with essentially zero initial kinetic energy are detected after passing through a 127° cylindrical plate analyzer. The nominal electron energy resolution is 25 meV as measured by the threshold photoelectrons from the $^2P_{3/2}$ state of Kr. The ion coincident with a given electron is measured with a time-of-flight mass spectrometer. The ion flight time is used as a measure of its mass. Since it is detected in coincidence with a threshold photoelectron, it is known that the internal energy of the parent molecule from which it came equals the photon energy ($h\nu$) minus the ionization potential (IP).

The light intensity is measured by the photocurrent from a tungsten electrode with a vibrating reed electrometer. The response of the detector was corrected by using the quantum yield curves obtained by Wheaton [16] for a tungsten surface of crystalline appearance. This curve was extended to 1300 Å by normalizing to the data of Cairns and Samson [17] at 1200 Å. The ratio of the quantum yield so obtained at 725 and 1300 Å was 15. This agrees with the ratio from the data of Cairns and Samson [17] but differs from the value of 8 given by Samson [18]. It is to be noted that the quantum yield, i.e. the relative light intensity, affects the TPES data but not the coincidence ion data since the coincidence ion data are simply the ratio of the number of coincidence ions of each mass divided by the total number of coincident ions detected.

The sample was obtained from commercial sources and had a stated purity of 97%. Gas chromatographic analysis showed a 0.4% propylene impurity. Presumably the other 2.6% impurity is propyne. Neither of these impurities should effect the data presented here since the fragmentation onsets from these impurities are higher than those from allene.

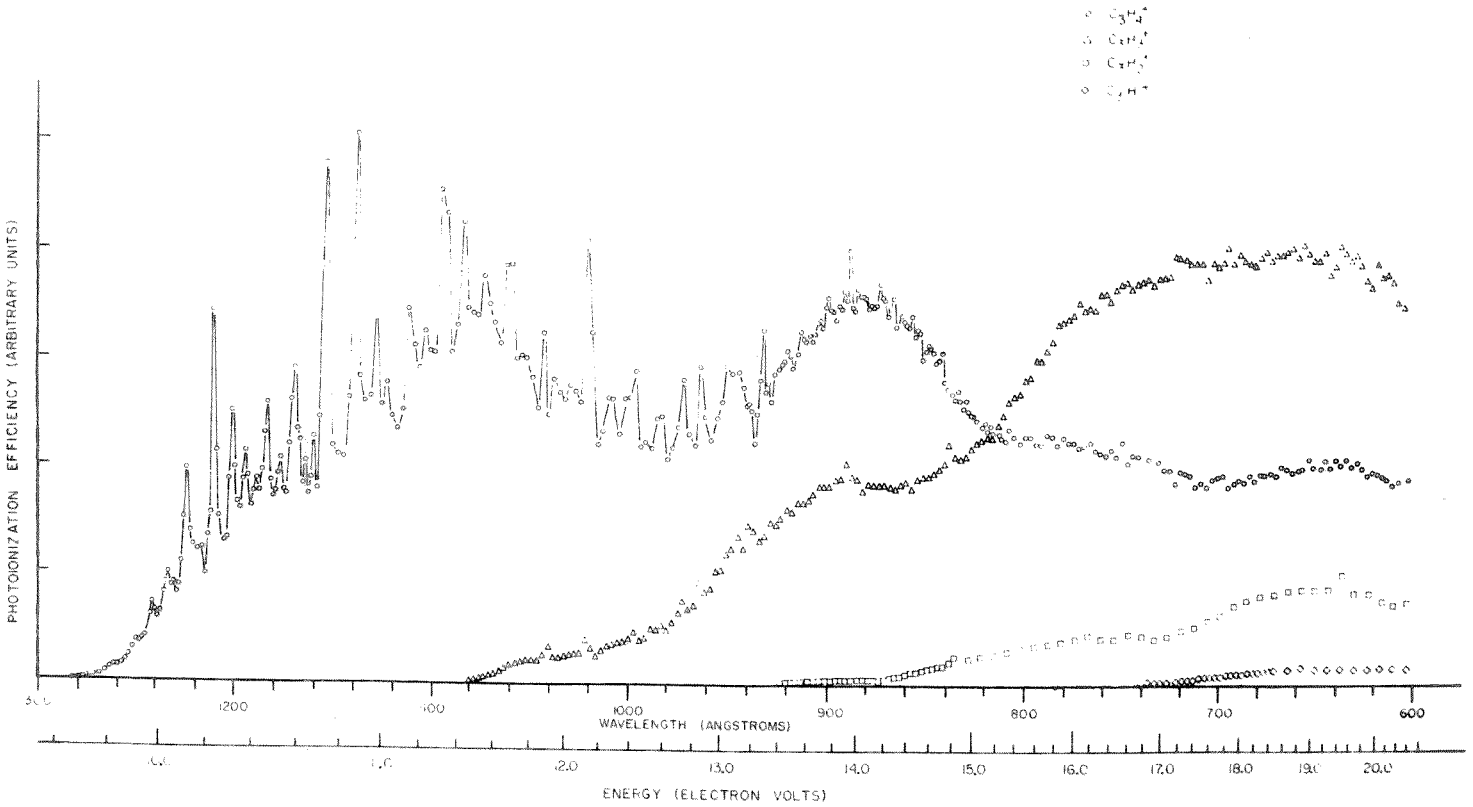

Fig. 1. Photoionization efficiency curve of allene and its fragment ions between thresnold and 600 Å. The ordinate is the photoionization efficiency in arbitrary untis. The abscissa is linear in wavelength given in Angstroms with a non-linear energy scale given in electron volts. The curves have been corrected to give the correct relative intensity of the parent ion and fragments.

RESULTS

The photoionization efficiency curves for the parent ion $C_3H_4^+$ and the fragments $C_3H_3^+$, $C_3H_2^+$ and C_3H^+ from threshold to 600 Å (20.6 eV) are given in Figs. 1 and 2. The curves of Fig. 1 are normalized to show the correct relative intensities. The abscissa has been plotted linear in wavelength since the resolution function of the monochromator is constant in wavelength. A nonlinear energy scale in electron volts is shown for convenience.

The TPES of allene is shown in Fig. 3(A). The data were obtained by counting threshold electrons for a fixed integrated light flux. Sample pressures were $1—3 \times 10^{-5}$ torr as measured by a hot cathode ionization gauge. Counting rates varied from 3 to 80 electrons per second. A background rate which has a maximum of 10% of the electron rate at 700 Å has been removed.

The TPES can be compared with the PES results of Baker and Turner [6] and Thomas and Thompson [7]. The relative intensity of the band at 10 eV and the band at 15 eV are similar in both the PES and the TPES. They both show two bands of equal height. Differences could be due to instrument effects in the PES experiment, such as changes in cross-section with energy above threshold, changing transmission of the electron energy analyzer with energy or changing angular distribution with energy. These factors, while important considerations for PES, do not affect the TPES experiments. Factors

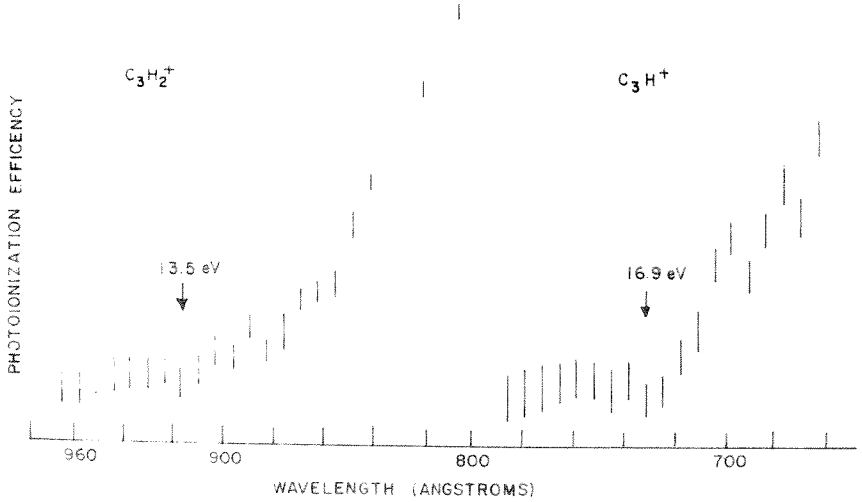

Fig. 2. Data in Fig. 1 with expanded scales to show the photoionization onsets of the $C_3H_2^+$ and C_3H^+ fragments. The relative intensity of the curves has not been maintained.

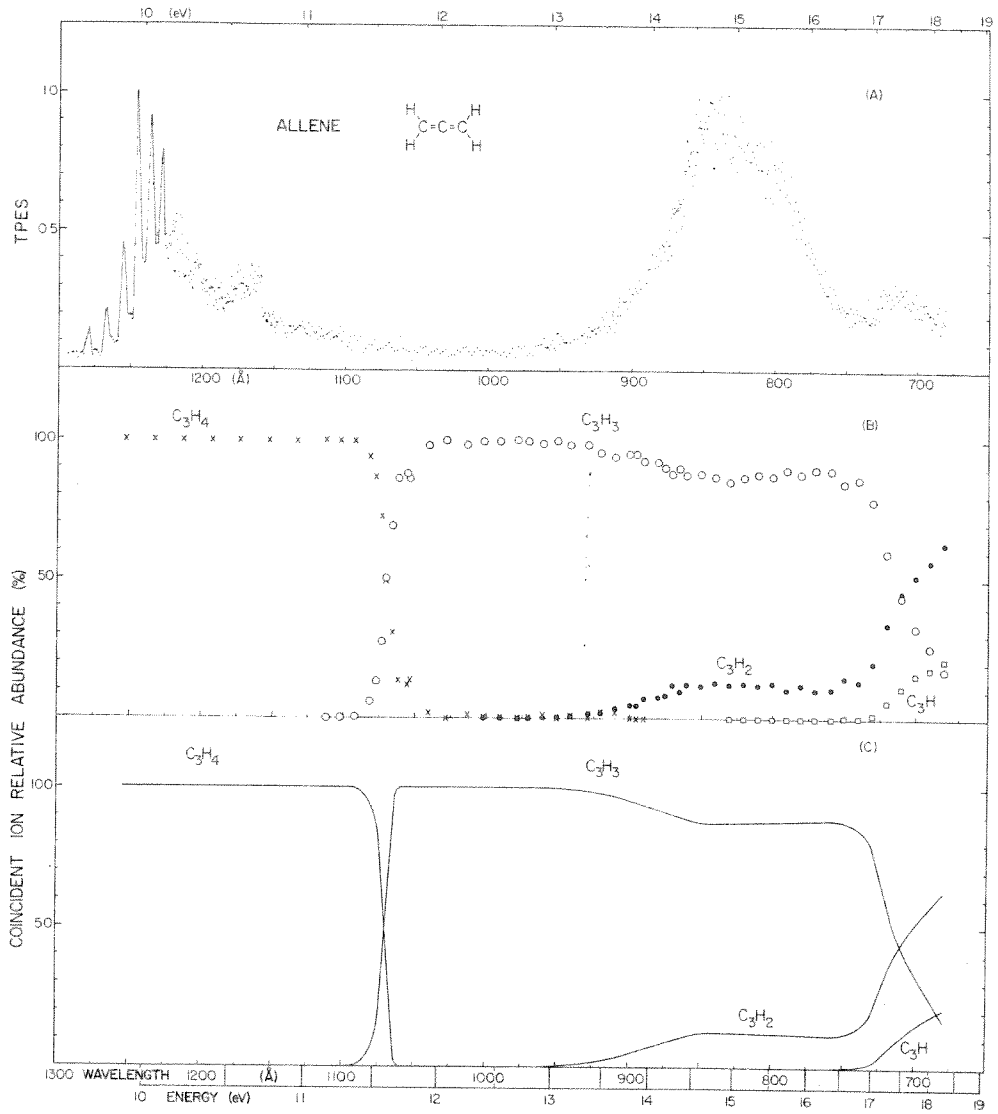

Fig. 3. (A) Threshold photoelectron spectra of allene from onset to 675 Å. The ordinate is electron rate per unit photon in arbitrary units and the abscissa is wavelength in Angstroms with a non-linear energy scale in electron volts. (B) Breakdown curve for allene and its fragments. The ordinate is relative coincident ion intensity and abscissa is wavelength in Angstroms. (C) Breakdown curve for allene. Same as 2 (B) except corrected for energy analyzer tailing and a smooth average line drawn through the data points.

which could affect the relative intensity in TPES include autoionization processes which produce near-zero energy electrons and improper correction for the relative quantum yield of the tungsten photodiode ligh detector.

The TPES data show considerable ionization 5—10-times background in the region between the two main bands, i.e. between 11 and 13.5 eV, while the PES data shows little if any ionization in this region. This implies that there are states in this region which autoionize and produce low-energy electrons which are detected as threshold photoelectrons by the instrument. The design of the electron analyzer ensures that the energy of these electrons is less than 300 meV. The existence of these autoionizing states is important for consideration of the fragmentation of the molecule.

The TPES data show a series of well isolated peaks starting at 1280 Å. The adiabatic ionization potential is 9.696 ± 0.002 eV. The position of the first six peaks, which are not obscured by autoionization, are in essential agreement with those reported by Thomas and Thompson [7]. There is some evidence for autoionization interference in the fifth and sixth peaks. They are slightly broader than the first four and there is a small peak in the valley between them.

The photoionization data and the coincidence data are inherently different. The photoionization fragment curves of Figs. 1 and 2 give the relative probability into which species a parent ion will fragment if it absorbs a photon of a particular enegy. These are termed the photoionization efficiency curves. The coincidence data given in Fig. 3(B) and (C) is the relative probability into which species a parent ion will fragment if it has a particular internal energy. These are termed the breakdown curves. Since the two kinds of data are different, we will for the most part discuss them separately in the next two sections.

PHOTOIONIZATION RESULTS

Parent ion $C_3H_4^+$

The parent ion onset is at 9.69 eV ± 0.01 eV. This differs slightly from previous photoionization results [8]. The intensity at threshold is down by a factor of ca. 500 from the maximum, and tails slightly, presumably owing to thermal excitation of the neutral molecule. The photoionization threshold was confirmed by TPES which shows an onset to within experimental error at the same energy. The relative intensities of the peaks in the TPES data show that if the onset were lower it would be observed. Hence, it is concluded that the observed onset at 9.69 eV is probably the adiabatic ionization potential. However, since 30% of the neutral molecules are thermally excited at room temperature, it is possible that the first one or two steps in the photoionization data and the corresponding peaks in the TPES and PES are due to ionization from these thermally excited neutral molecules.

Matthews and Warneck [9] report a photoionization value of 9.53 eV for the adiabatic ionization potential. This value, 0.16 eV lower than the present work or the photoelectron values [6,7] is outside the experimental

error reported. Since Matthews and Warnick did not report their data, resolution of the discrepancy is difficult. It would seem unlikely that this difference is due to thermal excitation of the neutral and must arise from other causes.

The data for the parent molecule show a great deal of structure that is due to autoionization. There are a series of steps from onset to ca. 9.95 eV which correspond to the first few vibrational peaks observed in the photoelectron studies and TPES study reported here. Above 9.95 eV the steps are completely masked by autoionization lines. The appearance of the autoionization at ca. 10 eV corresponds with the disruption of the TPES data at the same energy. The intensity of autoionizing lines reaches a local maximum at ca. 11.4 eV (1090 Å). The curve again maximizes at 14.0 eV (880 Å) with strong bunching of lines.

The major lines observed and their energies are listed in Table 1. Relative intensities are not listed as the data were taken in this region (i.e. energy less than 13.4 eV) with the hydrogen many-line spectrum. Although the hydrogen many-line spectrum can be considered to be quasicontinuous owing to the density of hydrogen lines and the spectral broadening arising

TABLE 1

Principal autoionization lines in allene

Wavelength [a]	E (cm^{-1})	Wavelength	E (cm^{-1})
1262	79210	1085	92200
1250	80000	1074	93140
1242	80530	1061	94220
1234	81060	1055	94830
1224	81700	1044	95830
1216	82250	1038	96330
1210	82620	1030	97100
1201	83280	1022	97880
1194	83750	1009	99070
1188	84140	1000	100010
1183	84530	985	101550
1176	85020	972	102840
1169	85510	964	103710
1160	86220	951	105200
1154	86630	948	105510
1139	87770	933	107210
1128	88630	920	108640
1123	89050	914	109450
1112	89930	900	111110
1104	90600	889	112480
1094	91390		

[a] Wavelength has been rounded to the nearest Angstrom.

from the light source conditions, the reliability of intensities of autoionizing lines measured with a line source is too uncertain to warrant presenting them here.

Some care was taken to determine what effect, if any, the light source and light detection system has on the structure observed. We could not establish any correlation between lines in the hydrogen spectra with the autoionization lines observed for allene. While there are some coincidences, as might be expected, for the most part no correlation was found between the hydrogen lines and the autoionization lines. In addition, the autoionizing structure persists in the region where the helium continuum was used.

Various operating conditions of the photomultiplier and various thicknesses of sodium salicylate were used to establish that the response of the light detection system was linear. The light intensities observed agree well with previous ones taken with other detectors such as metal surface photoelectric detectors.

Below 825 Å the parent curve is fairly smooth. There is no direct observation of the state observed by Baker and Turner [6] and Thomas and Thompson [7] at ca. 17.5 eV.

The lines for the most part lie above the ionization limits, as measured by photoelectron spectroscopy or absorption spectroscopy. These transitions therefore must be Rydberg transitions which autoionize and which have as their limit an excited state of the ion. This interpretation is suggested by the bunching of lines, some of which are unresolved, at ca. 14 eV. Baker and Turner [6] report what is presumably an adiabatic ionization energy at 14.1 eV and a vertical ionization energy at 14.9 eV. Thomas and Thompson [7] report a vertical ionization energy of 14.75 eV, which presumably refers to the same state.

The ground state of allene is of D_{2d} symmetry and the electron configuration of the ground state is $(1a_1)^2(1b_2)^2(2a_1)^2(3a_1)^2(2b_2)^2(4a_1)^2(3b_2)^2(1e)^4$-$(2e)^4$. Molecular orbital calculations have been made by a number of authors [19—21] and Rydberg-state calculations on the neutral molecule have been performed by Betts and McKoy [5]. Schaad et al. [20] calculate inner orbital transitions such as $1e \rightarrow 3e$. Some of these transitions lie in the energy region observed here and could possibly account for some of the structure observed. The lines observed here must arise from either promotion of 2 ($2e$) electrons or promotion of an inner orbital such as the ($1e$). Schaad et al. also calculate the expected states that arise from the D_{2h} (planar) symmetry of the allene molecule and give correlations to the D_{2d} states. It is likely that one or more of the states discussed by Schaad et al. are the first members of the Rydberg progressions we observed.

The autoionization structure is complex. Lack of well defined band envelopes and the apparent overlap of several series preclude any simple analysis of the autoionization lines. One possible set of assignments is given in Table 2. The first band would consist of the first four major lines above 10 eV. It is noted that the separation of the first two levels is ca. 900 cm^{-1} and level

Table 2

Autoionization bands observed near threshold in allene

Wavelength	Energy (cm^{-1})	Difference	Rydberg denominator
1st band			
1224	81700	920	
1210	82620	660	
1201	83280	470	1.7
1194	83750		
2nd band			
1169	85510	1120	
1154	86630	1140	1.84
1139	87770	860	
1128	88630		

separations decrease with increasing energy. If one takes as the limit for these lines the state with a vertical ionization potential at 14.9 eV, a Rydberg denominator of $(n - \sigma) = 1.70$ is obtained. Hence, the next band would then be expected at ca. 105,000 cm^{-1} (13.02 eV). If the broad peak at 105,500 cm^{-1} (13.08 eV) is taken as the second member of this series one obtains a Rydberg denominator of 2.73. The third member would probably be the line at 112,140 cm^{-1} (13.90 eV) giving a Rydberg denominator of 3.69.

A second band starting at 1169 Å is listed in Table 2. Assuming this is the first member of a Rydberg series with a limit of 14.9 eV, the Rydberg denominator is 1.83. The second member of the series should lie at ca. 107,000 cm^{-1} (13.27 eV). The line at 107,210 cm^{-1} (13.29 eV) is a likely choice giving a Rydberg denominator of 2.91. The third member should lie about 113,000 cm^{-1} (14.01 eV). There are lines in this region which are attributable to this interpretation.

The other lines observed between 11.0 eV and 12.0 eV are probably due to other states which have their limit as the 14.9-eV level or even the 15.4-eV level found by Baker and Turner. The lack of resolution of upper members of the series, however, makes interpretation impractical.

These assignments are meant to be purely suggestive. Surely other combinations and series can be found in the data which when properly analyzed will give a clear picture of the allene molecule in these higher states. A complete analysis of the autoionization is beyond the scope of this paper.

The weakness of the adiabatic transition compared to the autoionization implies that the ground state of the molecular ion is of a different configuration and perhaps different symmetry than that of the ground state of the neutral molecule. A likely possibility is that the molecular ion could have D_{2h} planar symmetry. The autoionizing states could retain the symmetry of

the neutral molecule and subsequently decay into states of the molecular ion.

Fragment ion $C_3H_3^+$

The $C_3H_3^+$ fragment ion has an appearance potential of 11.48 ± 0.02 eV. This value agrees with the previous photoionization results [8,9] and the electron monochromator study by Lossing [10]. Ignoring the thermal shift and kinetic shift which tend to cancel, one obtains a value of the heat of formation for the $C_3H_3^+$ ion of ca. 1084 kJ mol^{-1} (259 kcal mol^{-1}) [22]. (The thermal shift will be discussed with the coincidence results.) Lossing has concluded that the $C_3H_3^+$ ion formed from allene at threshold is the cyclopropenyl ion. His direct measurement of the ionization potential of the propargyl radical determines its heat of formation to be near 1176 kJ mol^{-1} (281 kcal mol^{-1}). This is too high for the fragment observed here by ca. 96 kJ mol^{-1} (23 kcal mol^{-1}), leaving the cyclopropenyl radical as the most likely structure formed since its heat of formation is ca. 1071 kJ mol^{-1} (256 kcal mol^{-1} [10]).

The $C_3H_3^+$ curve rises gradually with some structure which correlates with autoionization lines in the parent. At ca. 12.5 eV there is a change in slope and a more rapid rise. It is possible this could represent the formation of $C_3H_3^+$ in the propargyl form as there is sufficient energy above 12.5 eV for this to occur. The curve levels off at ca. 13.9 eV. At 14.6 eV it again rises and by 15.3 eV the $C_3H_3^+$ ion is more intense than the parent. Above 16.4 eV the curve is approximately horizontal. The rise at 14.6 eV is due presumably to the contribution of the excited state of the parent ion at about this energy. Ignoring thermal and kinetic shifts, the bond energy for H loss from $C_3H_4^+$ is ca. 1.8 eV.

Fragment ion $C_3H_2^+$

The $C_3H_2^+$ fragment has an appearance potential of 13.5 ± 0.2 eV. This is 0.9 eV lower than the electron impact value of 14.34 eV reported by Franklin and Mogenis [11]. We observed the intensity at threshold to be very weak. At ca. 14.2 eV the curve breaks upward and starts leveling off at ca. 15.5 eV and the curve has another upward break at ca. 17.1 eV. All the fragment curves show an increase at about this energy, which could be due to the state of the ion at 17.4 eV reported by Baker and Turner [6]. The increase of intensity of the $C_3H_2^+$ and C_3H^+ ions above 17.1 eV accounts for the leveling off of the $C_3H_3^+$ curve.

Assuming $C_3H_2^+$ is formed in the reaction

$$C_3H_4 + h\nu \rightarrow C_3H_2^+ + H_2 + e^-$$

$\Delta H_f(C_3H_2^+)$ = 1494 kJ mol^{-1} (357 kcal mol^{-1}). Kinetic and thermal shifts have been ignored. For a competing process such as this, the kinetic shift is expected to be larger than the thermal shift making this an upper limit to the heat of formation. This upper limit is lower than those observed in electron

impact studies [11,23]. The difference between the appearance potential of $C_3H_3^+$ and $C_3H_2^+$ can be considered to be a measure of the bond energy of a hydrogen on the $C_3H_3^+$ molecule. This difference is 2.0 eV.

Fragment ion C_3H^+

C_3H^+ has an appearance potential of 16.9 ± 0.2 eV. It, like the $C_3H_2^+$ ion, has a very weak intensity at threshold. This value is 1.8 eV less than the value reported by Franklin and Mogenis [11]. At ca. 17 eV the C_3H^+ curve takes an upward break and is essentially constant beyond 18.4 eV. Assuming the reaction for the formation of C_3H^+ is

$$C_3H_4 + h\nu \rightarrow C_3H^+ + H_2 + H + e^-$$

an upper limit of $\Delta H_f(C_3H^+) \leqslant 1594$ kJ mol^{-1} (381 kcal mol^{-1}) is established for the heat of formation of the species. Values derived from electron impact data on allene, propyne and propylene range from 1465 to 1780 kJ mol^{-1} (350—425 kcal mol^{-1}). However, values derived from electron impact data on 1-buten-3-yne, 1,3-butadiene, and 1-butyne are less than 1255 kJ mol^{-1} (300 kcal mol^{-1}) *. Since the onset for C_3H^+ from each of the C_3 compounds is near an excited electronic state of the parent ion (ca. 17.5 eV), the question arises whether this fragment is formed exclusively from this electron state. The observation in the electron impact mass spectrum [24] of a metastable ion (apparent mass 35) corresponding to the secondary process $C_3H_3^+ \rightarrow C_3H^+ + H_2$ indicates the fragment is not coming from an excited state of the parent. The difference between the two heats of formation may be due to two different structures of C_3H^+.

COINCIDENCE RESULTS

The threshold photoelectron coincident ion data are shown in Fig. 3(B). These are the number of coincident ions of each mass divided by the total number of coincident ions. Hence, these ratios are independent of sample pressure, light intensity (and therefore the quantum yield of the photodetector) and counting time. Scattered light and accidental coincidence backgrounds amounting to ca. 5% have been removed from the data. The tail of the parent ion curve above the onset of the first fragment has been shown [25] to be due primarily to the high-energy tailing of the electron energy analyzer. Therefore the data in Fig. 3(B) have been reworked by drawing smooth lines between the points and eliminating most of the parent ion high energy tail. The result is shown in Fig. 3(C). These are the breakdown curves and are important experimental data to compare with calcula-

* Dr. F.P. Lossing (private communication) has recently measured the appearance potential of C_3H^+ from 1,3-butadiene to be 18.7 eV. This is considerably higher than previous measurements and may indicate that the low heat of formation of C_3H^+ from 1-butene-3-yne and 1-butyne are also erroneous.

tions based upon quasi-equilibrium theory of unimolecular dissociation (QET) [12]. Calculated breakdown curves for allene are unavailable in the literature so a direct comparison with the prediction of QET is impossible. However, the general predictions of QET where appropriate will be referred to in the discussion of the breakdown curves.

One of the most interesting features of the breakdown curves is that the onset of the first fragment occurs in a region where there is little or no direct ionization as shown by PES. The parent ions formed in this energy region, 11 eV → 13 eV, are formed primarily by autoionization processes. Some of this autoionization leads to low-energy and zero-energy electrons which are detected in the coincidence experiment. The internal energy of the parent ions from these processes is still $h\nu - IP$ to within the energy resolution of the electron analyzer. The fragmentation from these parent ions appears to be consistent with QET.

Another important point is that the appearance potentials of the fragment processes obtained from the breakdown curves are lower than those obtained in the photoionization data. Both sets of appearance potentials are given in Table 3 and compared with previous work. The tails of the fragment onsets in the breakdown curves extrapolate to a lower energy in each case, but in particular with the $C_3H_2^+$ and C_3H^+ fragments. The reason for this is probably due to different instrumental sensitivities and different instrumental sampling time. The sampling time is the maximum time between ion production and fragmentation that the ion can still be detected as a fragment. In the photoionization experiment, this time is determined by the ion drawout voltage and is probably 0.1—0.5 μs. In the coincidence

TABLE 3

Appearance potentials in electron volts for the parent and fragment ions of allene

This work			Other work		
Ion	Photoionization	Coincidence	Value	Method[a]	Ref.
$C_3H_4^+$	9.69 ± 0.01	9.696 ± 0.002	9.62 ± 0.04	PI	8
			9.53 ± 0.03	PI	9
			9.69	PE	6
			9.68	PE	7
			9.62	EM	10
$C_3H_3^+$	11.48 ± 0.02	11.37 ± 0.02	11.48 ± 0.02	PI	8
		11.68 ± 0.03[b]	11.48 ± 0.03	PI	9
			11.47	EM	10
$C_3H_2^+$	13.5 ± 0.2	13.0 ± 0.1			
C_3H^+	16.9 ± 0.1	16.5 ± 0.2			

[a] PI = photoionization; PE = photoelectron spectroscopy; EM = monochromatic electron impact.

[b] Value corrected for thermal energy.

experiment, this time is ca. 2 μs and is determined by the delay time between production of the ion and application of the ion drawout field. The longer sampling time in the coincidence experiment allows fragments to be detected at lower energies.

The width of the crossover between the parent ion and the first fragment ($C_3H_3^+$ for allene) is in general due to initial thermal excitation of the parent molecule and the change with energy in the rate constant for forming the fragment. The thermal energy shifts the fragment onset toward lower energy (thermal shift) while the change in rate constant shifts the onset toward higher energy (kinetic shift). The extrapolation of the parent ion curve to zero abundance gives the energy where all the parent ions have fragmented. Hence, this is the energy where parent molecules with no initial thermal energy have fragmented and corresponds to the zero Kelvin onset for the fragmentation. This value, given in Table 3, is still an upper limit since it has not been corrected for kinetic shift.

The breakdown curves give a clear picture of the fragmentation of the allene molecular ion. When the internal energy ($=h\nu - IP$) is ca 1.8 eV the parent ion has enough energy to fragment by losing an H atom to form $C_3H_3^+$. Once this energy is exceeded fragmentation is complete and no parent ions remain (parent ions are still produced at photon energies greater than this, but some of the photon energy is carried off by the electron.) In the threshold region the $C_3H_3^+$ ion comes from states of the $C_3H_4^+$ parent formed by autoionization. Since the $C_3H_3^+$ ion at threshold is thought to have the cyclopropenyl structure it would seem likely that the $C_3H_4^+$ states which result from the autoionization are of a configuration to make this reaction proceed easily. In this region the electron comes from one of the carbon double bonds. The high internal energy of the molecular ion could presumably lead to bending and distortion which makes formation of the cyclopropenyl structure with the consequent hydrogen rearrangement a favorable process.

The $C_3H_2^+$ formation via H_2-loss from the parent starts in the region above 13 eV. The $C_3H_2^+$ curve rises slowly to ca. 14.5 eV. Corresponding to this rise is the decrease in the $C_3H_3^+$ curve as a result of competition between the two processes. Above 14.5 eV, there is a slight (1—2%) decrease in the $C_3H_2^+$ curve. This decrease in the absence of a new competing fragmentation is not possible under QET. The decrease could be due to a low probability process such as fluorescence by which the parent ion loses some of its energy before fragmentation. Also, if the H_2-loss occurs with a larger kinetic energy release than the H-loss, the decrease could be due to increased discrimination in the TOF mass analyzer against the higher kinetic energy fragment. Above 17 eV the $C_3H_2^+$ curve suddenly increases. This is presumably due to the secondary process, H-loss from $C_3H_3^+$. Also near 17 eV the C_3H^+ curve rises rapidly, presumably owing to secondary process, H_2-loss from $C_3H_3^+$.

As discussed in the photoionization section of this paper the close coincidence in energy of the second break in the $C_3H_2^+$ curve and the onset of

C_3H^+ formation could be due to fragmentation directly from the excited state of the ion which has its onset at ca. 17 eV. If this is so, parent ions initially in this state would preferentially fragment to $C_3H_2^+$ and C_3H^+ rather than $C_3H_3^+$. The observation of the metastable process for $C_3H_3^+ \rightarrow C_3H^+ + H_2$ rules out this possibility for C_3H^+. The metastable process for $C_3H_3^+ \rightarrow C_3H_2^+$ would have an apparent mass of 37.03 and would normally be obscured by the large normal mass 37 peak. Assuming the increased production of $C_3H_2^+$ at 17 eV is due to the loss of H from $C_3H_3^+$, one can conclude from the similar energy onsets that the same energy is required to remove H and H_2 from $C_3H_3^+$. However, the H and H_2 may be coming from different isomeric forms of $C_3H_3^+$.

CONCLUSIONS

The absorption of light by allene above the ionization potential is dominated by autoionization processes. Fragmentation proceeds from the states which result from the autoionization process. A fraction of the excited states of the neutral species which are formed and subsequently decay to an ion and free electron, decay with small amounts of energy released to the electron. This is indicated by the TPES data as compared to published PES data. In fact, in the threshold region of the $C_3H_3^+$ fragment these states are largely responsible for the fragmentation process. A qualitative interpretation of the autoionizing structure has been given here. Calculations coupled with perhaps higher resolution data would be of benefit to completely understand the ionization.

The adiabatic ionization potential measured here by two independent techniques is 9.69 ± 0.01 eV. This agrees well with recent PES studies, but may include contributions from thermally excited neutral species. The remeasurement of the heat of formation of the $C_3H_3^+$ ion confirms previous measurements and supports Lossing's [10] conclusion that the cyclopropenyl structure is formed at threshold. Upper limits to the heats of formation of the $C_3H_2^+$ and C_3H^+ ions from allene have been determined. The values of 1494 kJ mol^{-1} (357 kcal mol^{-1}) and 1594 kJ mol^{-1} (381 kcal mol^{-1}), respectively, are probably accurate to within 33 kJ mol^{-1} (8 kcal mol^{-1}).

ACKNOWLEDGMENTS

The authors wish to thank Drs. Henry M. Rosenstock and Kenneth McCulloh for helpful discussions and suggestions concerning the manuscript. The work at the University of Alabama was supported in part by Grant AFOSR 74-2726 and in part by the Research Grants Committee of the University of Alabama.

REFERENCES

1 L.H. Sutcliffe and A.D. Walsh, J. Chem. Soc. (London), (1952) 899.
2 A.A. Iverson and B.R. Russell, Spectrochim. Acta, Part A, 28 (1972) 447.
3 J.W. Rabalais, J.M. McDonald, V. Scherr and S.P. McGlynn, Chem. Rev., 71 (1971) 73.
4 G. Herzberg, Molecular Spectra and Molecular Structure II, Electronic Spectra and Electronic Structure of Polyatomic Molecules, D. Van Nostrand Co., Princeton, N.J., 1966.
5 T.C. Betts and V. McKoy, J. Chem. Phys., 60 (1974) 2947.
6 C. Baker and D.W. Turner, Chem. Commun., (1969) 480.
7 R.K. Thomas and H. Thompson, Proc. Royal Soc., Ser. A, 339 (1974) 29.
8 A.C. Parr and F.A. Elder, J. Chem. Phys., 49 (1968) 2659.
9 C.S. Matthews and P. Warneck, J. Chem. Phys., 51 (1969) 854.
10 F.P. Lossing, Can. J. Chem., 50 (1972) 3973.
11 J.L. Franklin and A. Mogenis, J. Phys. Chem., 71 (1967) 2820.
12 M.B. Wallenstein, A.L. Wahrhaftig, H.M. Rosenstock and H. Eyring, Oberlin Symposium on Radiobiology, June 1950, Wiley, New York; H.M. Rosenstock, M.B. Wallenstein, A.L. Wahrhaftig and H. Eyring, Proc. Nat. Acad. Sci. U.S.A., 38 (1952) 667. For a more recent review see H.M. Rosenstock, in E. Kendrick (Ed.), Advances in Mass Spectroscopy, Vol. 4, Institute of Petroleum, London, 1968, p. 523.
13 R. Stockbauer, J. Chem. Phys., 58 (1973) 3800; R. Stockbauer and M.G. Inghram, J. Chem. Phys., 65 (1976) 4081; A.S. Werner, B.P. Tsai and T. Baer, J. Chem. Phys., 60 (1974) 3650; J.H.D. Eland, Int. J. Mass Spectrom. Ion Phys., 8 (1972) 143.
14 R. Stockbauer, Int. J. Mass Spectrom. Ion Phys., 25 (1977) 89.
15 W.C. Wiley and I.H. McLaren, Rev. Sci. Instrum., 26 (1955) 1150.
16 J.E.G. Wheaton, J. Opt. Soc. Am., 54 (1964) 1287.
17 R.B. Cairns and J.A.R. Samson, J. Opt. Soc. Am., 56 (1966) 1568.
18 J.A.R. Samson, Techniques of Vacuum Ultraviolet Spectroscopy, John Wiley, New York, 1967, p. 231.
19 W. Runge, W. Kosbahn and J. Kroner, Ber. Bunsenges. Phys. Chem., 79 (1975) 371.
20 L.J. Schaad, L.A. Burnelle and K.P. Dressler, Theor. Chim. Acta, 15 (1969) 91.
21 References 3, 19, and 20 contain references to other theoretical calculations done on the allene molecule.
22 The heats of formation of the neutral species were taken from ref. 23.
23 H.M. Rosenstock, K. Draxl, B.W. Steiner and J.T. Herron, J. Phys. Chem. Ref. Data, 6 (1977) Supplement 1.
24 Catalog of Mass Spectral Data, American Petroleum Institute, Project 44, 1954, pp. 1134, 1135.
25 R. Stockbauer and M.G. Inghram, J. Chem. Phys., 62 (1975) 4862.